British Journal of Pharmacology (2001) 134, 1215–1226

www.nature.com/bjp

Pharmacological and biochemical characterization of adenosine receptors in the human malignant melanoma A375 cell line

[1]Stefania Merighi, [1]Katia Varani, [1]Stefania Gessi, [1]Elena Cattabriga, [1]Valeria Iannotta, [2]Canan Ulouglu, [3]Edward Leung & *,[1]Pier Andrea Borea

[1]Department of Clinical and Experimental Medicine, Pharmacology Unit, University of Ferrara, Centro Nazionale Di Eccellenza Per Lo Sviluppo Di Metodologie Innovative Per Lo Studio Ed Il Trattamento Delle Patologie Infiammatorie, Italy; [2]Department of Pharmacology, Gazi University, Medical Faculty, Ankara, Turkey and [3]King Pharmaceuticals, Cary, North Carolina, U.S.A.

1 The present work characterizes, from a pharmacological and biochemical point of view, adenosine receptors in the human malignant melanoma A375 cell line.

2 Adenosine receptors were detected by RT–PCR experiments. A_1 receptors were characterized using [^{3}H]-DPCPX binding with a K_D of 1.9 ± 0.2 nM and B_{max} of 23 ± 7 fmol mg^{-1} of protein. A_{2A} receptors were studied with [^{3}H]-SCH 58261 binding and revealed a K_D of 5.1 ± 0.2 nM and a B_{max} of 220 ± 7 fmol mg^{-1} of protein. A_3 receptors were studied with the new A_3 adenosine receptor antagonist [^{3}H]-MRE 3008F20, the only A_3 selective radioligand currently available. Saturation experiments revealed a single high affinity binding site with K_D of 3.3 ± 0.7 nM and B_{max} of 291 ± 50 fmol mg^{-1} of protein.

3 The pharmacological profile of radioligand binding on A375 cells was established using typical adenosine ligands which displayed a rank order of potency typical of the different adenosine receptor subtype.

4 Thermodynamic data indicated that radioligand binding to adenosine receptor subtypes in A375 cells was entropy- and enthalpy-driven.

5 In functional assays the high affinity A_{2A} agonists HE-NECA, CGS 21680 and $A_{2A}-A_{2B}$ agonist NECA were able to increase cyclic AMP accumulation in A375 cells whereas A_3 agonists Cl-IB-MECA, IB-MECA and NECA were able to stimulate Ca^{2+} mobilization.

6 In conclusion, all these data indicate, for the first time, that adenosine receptors with a pharmacological and biochemical profile typical of the A_1, A_{2A}, A_{2B} and A_3 receptor subtype are present on A375 melanoma cell line.

British Journal of Pharmacology (2001) **134,** 1215–1226

Keywords: Adenosine receptors; A375 melanoma cell line; cyclic AMP; calcium levels; thermodynamic studies

Abbreviations: CGS 15943, 5-amino-9-chloro-2-(furyl)1,2,4-triazolo[1,5-c] quinazoline; CGS 21680, (2-[p-(2-carboxyethyl)-phenethyl-amino]-5′-N-ethyl-carboxamidoadenosine); CHA (N^6-cyclohexyladenosine), ClIBMECA N^6 (3iodobenzyl) 2chloroadenosine 5′- N-methyluron-amide; CPA, N^6-cyclopentyladenosine, CPT, 8-cyclopentyltheophylline; DPCPX, 1,3-dipropyl-8-cyclopentyl-xanthine; [^{3}H]-DPCPX, 1,3dipropyl8cyclopentylxanthine; HENECA, (2-hexynyl-5′Nethylcarboxamidoadenosine); [^{3}H]-MRE 3008F20, [^{3}H]5-*N*-(4-methoxyphenylcarbamoyl)amino-8-propyl-2-(2-furyl) pyrazolo [4,3e]1,2,4triazolo [1,5c] pyrimidine; [^{3}H]-SCH58261, 5amino7 (2phenylethyl) 2 (2furyl) pyrazolo [4,3e] 1,2,4triazolo[1,5c] pyrimidine; IBMECA, N^6 (3iodobenzyl)-adenosine-5′-N-methyluronamide; MECA, 5′-(N-methyl)carboxamidoadenosine; MRE3008F20, 5*N*(4methoxyphenyl-carbamoyl)amino-8-propyl-2(2furyl)-pyrazolo[4,3e]1,2,4-triazolo[1,5-c] pyrimidine; MRE 3046F20, 5-*N*-(4-metylphenyl-carbamoyl)amino-8-metyl-2(2furyl)-pyrazolo-[4,3e]-1,2,4-triazolo[1,5-c]pyrimidine; MRE 3048F20, 5-*N*-(4phenylcarbamoyl)amino-8-ethyl-2(2furyl)-pyrazolo-[4,3e]-1,2,4-triazolo[1,5-c]pyrimidine; MRE 3055F20, 5-*N*-(4phenylcarbamoyl)amino 8 propyl 2 (2furyl) pyrazolo[4,3e]1,2,4triazolo[1,5c]pyrimidine; MRE 3062F20, 5-*N*-(4-phenylcarbamoyl)amino-8-butyl-2(2furyl)-pyrazolo-[4,3e]-1,2,4 triazolo[1,5-c]pyrimidine; NECA, 5′-N(ethyl)carboxamidoadenosine; 8-PT, 8phenyltheophylline; R-PIA, R(−)-N^6(2-phenyl-isopropyl)-adenosine; SCH58261,7-(2-phenylethyl)-2-(2furyl) pyrazolo [4,3*e*]1,2,4triazolo [1,5*c*]pyrimidine; S-PIA, S(−)N^6(2phenylisopropyl) adenosine

Introduction

Adenosine acts as an autacoid *via* interaction with four types of G protein-coupled receptors, termed A_1, A_{2A}, A_{2B} and A_3. These receptors are widely distributed in human body regulating virtually the function of every organ and tissue (Fredholm *et al*., 1994). They differ by their affinity for the endogenous agonist as well as by their pharmacological specificity. A_1, A_{2A} and A_3 receptors are activated by submicromolar concentrations of adenosine, whereas only the A_{2B} receptor appears to be activated when adenosine levels raise into the micromolar range (Fredholm *et al*., 2001).

*Author for correspondence at: Department of Clinical and Experimental Medicine-Pharmacology Unit, Via Fossato di Mortara 17-19, 44100 Ferrara, Italy; E-mail: bpa@dns.unife.it

In addition, adenosine receptors operate through distinct signalling mechanisms. The A_1 and A_3 subtypes control most, if not all, their cellular effectors *via* pertussis toxin-sensitive G proteins of the G_i and G_o family; in contrast, both A_{2A} and A_{2B} subtypes couple to G_s and thereby stimulate cyclic AMP formation (Ralevic & Burnstock, 1998). In particular, stimulation of A_3 receptors induces an intracellular signalling that actives phospholipase C and D and increases calcium concentrations (Olah & Stiles., 1995; Abbracchio *et al*., 1995). Adenosine has been linked to a variety of physiological processes, including mast-cell mediation of hypotension (Fozard *et al*., 1996; Guieu *et al*., 2001), induction of apoptosis (Yao *et al*., 1997; Schrier *et al*., 2001), inhibition of tumour necrosis factor α production from macrophage-like cell line (Elenkov *et al*., 2000), inhibition of platelet-activating factor-induced chemotaxis of human eosinophils (Walker *et al*., 1997), neural and cardiac protection (Liang & Jacobson., 1998; Safran *et al*., 2001) and depression of locomotor activity (Jacobson *et al*., 1993; Marston *et al*., 1998). Increased concentrations of adenosine have been detected in the absence of adenosine deaminase activity (ADA) (Blackburn *et al*., 1996) or under hypoxic conditions, e.g. large solid tumours (Blay *et al*., 1997). The mechanisms of adenosine effects on different tumoural tissues have not yet been carefully explored. Adenosine analogues are also used as pharmacological agents (Olah & Stiles., 1995). In particular adenosine, acting at specific A_{2A} receptors, promotes wound healing in both normal animals and in animals with impaired wound healing (Montesinos *et al*., 1997). Furthermore, adenosine stimulates angiogenesis in the dermis leading to improvement in function and appearance of the epidermis. Adenosine may also increase collagen and glicosaminoglycan production from fibroblasts and it is readily taken up by the cells (Ethier *et al*., 1993; Ethier & Dobson, 1997). In view of these hallmarks, clarification of the cellular and biochemical mechanisms of adenosine may be important for the understanding of its possible role in the pathogenesis of tumours of the skin, as basal cell carcinoma, squamous cell carcinoma, melanoma. Malignant melanoma is a serious form of skin cancer. Unfortunately, the incidence of this disease appears to be increasing, such that currently about 1 in 100 persons in the United States can expect to develop this cancer in a lifetime (Ariza *et al*., 1999). Recent advances in the understanding of extracellular adenosine-mediated transmembrane signalling through adenosine receptors together with the availability of molecular tools to study adenosine receptors will allow more detailed and precise evaluation of the effects of extracellular adenosine under well controlled conditions. To our knowledge, a complete investigation on adenosine receptors in tumours of the skin is not available. Prompted by these observations we performed, for the first time, a pharmacological and biochemical characterization of adenosine receptors in a human malignant melanoma cell line, A375. Adenosine receptors messengers (mRNA) were first revealed by RT–PCR experiments and then characterized by radioligand binding assays by using the selective A_1-, A_{2A}-, A_3-antagonists [^{3}H]-DPCPX, [^{3}H]-SCH 58261 and [^{3}H]-MRE 3008F20, respectively. The lack of available selective radioligands has until now hindered characterization of the A_3 receptors in any tissue. Thus, this newly developed antagonist radioligand represents a major contribution to the study of this receptor subtype (Varani *et al*., 2000a). Moreover, the abilities of typical A_{2A} and A_{2B} agonists to increase the cyclic AMP intracellular levels has been evaluated as well as the effect of high affinity A_3 agonists, such as Cl-IB-MECA, IB-MECA and NECA, in the induction of Ca^{2+} release. Finally, with the aim of obtaining new insights into the forces driving the coupling of adenosine receptors in human melanoma with selective ligands, a thermodynamic analysis of [^{3}H]-DPCPX, [^{3}H]-SCH 58261 and [^{3}H]-MRE 3008F20 binding has been performed and the enthalpic (ΔH°) and entropic (ΔS°) contribution to the standard free energy (ΔG°) of the binding equilibrium were determined.

Methods

Drugs

[^{3}H]-DPCPX (specific activity 120 Ci mmol^{-1}) was purchased from NEN Research Products (Boston, MA, U.S.A.). [^{3}H]-SCH 58261 (specific activity 68 Ci mmol^{-1}) was a kind gift of Dr E. Ongini, Schering-Plough Research Institute (Milan, Italy). CPA, MECA, CPT, 8PT, CGS 21680, CHA, NECA, R-PIA, S-PIA, C1-IB-MECA, IB-MECA, CGS 15943, DPCPX were obtained from Research Biochemical International (Natick, MA, U.S.A.). HE-NECA was a kind gift of Prof G. Cristalli, Dipartimento di Scienze Chimiche, University of Camerino, Italy. SCH 58261, MRE 3055F20, MRE 3062F20, MRE 3048F20, MRE 3046F20, MRE 3008F20 were synthesized by Prof P.G. Baraldi, Dipartimento di Scienze Farmaceutiche, University of Ferrara, Italy. MRE 3008F20 was successively labelled for us with ^{3}H-isotope ([^{3}H]-MRE 3008F20, specific activity 67 Ci mmol^{-1}, as previously described by Baraldi *et al*., 2000) at Amersham International (Buckinghamshire, U.K.). All other reagents were of analytical grade and obtained from commercial sources.

Cell culture

A375 cells (obtained from ATCC) were grown adherently and maintained in Dulbecco's Modified Eagle's Medium (DMEM), containing 10% foetal calf serum, penicillin (100 u ml^{-1}), streptomycin (100 μg ml^{-1}), L-glutamine (2 mM) at 37°C in 5% CO_2/95% air. Cells were split two or three times weekly at a ratio between 1 : 5 and 1 : 10.

RT–PCR

Total cytoplasmic RNA was extracted from 10^7 cells by the acid guanidinium thiocyanate phenol method. The human A_1 adenosine receptor sequence was amplified with 5′ primer sequence (GGA TGC CAC CTT CTG CTT CAT) and 3′ primer sequence (CTC GAA CTC GCA CTT GAT CAC) giving a 394 bp product. The human A_{2A} adenosine receptor sequence was amplified with 5′ primer sequence (GGG GTA CCA GTG GAG GGA GTG C) and 3′ primer sequence (AAG CCG CGG AGA AAG ATA AAG A) giving a 208 bp product. The human A_{2B} adenosine receptor sequence was amplified with 5′ primer sequence (ACG GTA CCA CAA GAA ACA AAG AGG AC) and 3′ primer sequence (AAG CCG CGG AGC CTA CTA CTG ACA) giving a 153 bp product. The human A_3 adenosine receptor sequence

was amplified with 5′ primer sequence (ACG GTG AGG TAC CAC AGC TTG TG) and 3′ primer sequence (ATA CCG CGG GAT GGC AGA CC) giving a 156 bp product. RT–PCR was carried out by using Access RT–PCR System (Promega), in 50 μl at the following conditions: first strand cDNA synthesis at 48°C for 45 min and 94°C for 2 min. Second strand cDNA synthesis and PCR amplification: 94°C for 30 s, 59.5°C (for A_1 and A_3) or 58.6°C (for A_{2A}) or 54°C (for A_{2B}) for 30 s and 68°C for 2 min (35–40 cycles). For β-actin amplification primers were as described elsewhere (Walther *et al*., 1994). Oligonucleotides were synthesized by M-Medical Genenco-Life Science, Florence, Italy. Subsequently, 10 μl of PCR products were run on the 2% agarose gel and visualized under u.v. illumination after ethidium bromide staining.

Membrane preparation

For membrane preparation the culture medium was removed. The cells were washed with PBS and scraped off T75 flasks in ice-cold hypotonic buffer (5 mM Tris HCl, 2 mM EDTA, pH 7.4). The cell suspension was homogenized with Polytron and the homogenate was spun for 10 min at $1000 \times g$. The supernatant was then centrifuged for 30 min at $100{,}000 \times g$. The membrane pellet was resuspended in 50 mM Tris HCl buffer pH 7.4 for A_1 adenosine receptors, 50 mM Tris HCl buffer pH 7.4, 10 mM $MgCl_2$ for A_{2A} adenosine receptors, 50 mM Tris HCl buffer pH 7.4, 10 mM $MgCl_2$, 1 mM EDTA for A_3 adenosine receptors and incubated with 3 IU ml^{-1} of Adenosine deaminase for 30 min at 37°C. Then the suspension was stored at −80°C. The protein concentration was determined according to a Bio-Rad method (Bradford, 1976) with bovine albumin as a standard reference.

Radioligand binding assays

Association kinetic studies of [^{3}H]-DPCPX (2 nM), [^{3}H]-SCH 58261 (4 nM) and [^{3}H]-MRE 3008F20 (4 nM) were performed incubating membranes obtained by A375 cells at 25°C for A_1 and at 4°C for A_{2A} and A_3, respectively. For the measurement of the association rate, the reaction was terminated at different times (from 5 to 200 min) by rapid filtration under vacuum, followed by washing with 5 ml ice-cold buffer four times. For dissociation studies, membranes were pre-incubated with [^{3}H]-DPCPX (2 nM), [^{3}H]-SCH 58261 (4 nM) and [^{3}H]-MRE 3008F20 (4 nM) at 25°C for A_1 and at 4°C for A_{2A} and A_3, respectively, for 150 min. Specific binding was then measured at 5–120 min after the addition of 1 μM DPCPX, SCH 58261 and MRE 3008F20 for A_1, A_{2A} and A_3, respectively. Saturation binding experiments of [^{3}H]-DPCPX, [^{3}H]-SCH 58261 and [^{3}H]-MRE 3008F20 to A375 cells were performed incubating membranes (100 μg of protein/assay) at 25°C for A_1 and at 4°C for A_{2A} and A_3, respectively, for 150 min. Competition experiments of 2 nM [^{3}H]-DPCPX, 4 nM [^{3}H]-SCH 58261 and 4 nM [^{3}H]-MRE 3008F20 were performed in duplicate in a final volume of 100 μl in test tubes containing 50 mM Tris HCl buffer (10 mM $MgCl_2$ for A_{2A}, 10 mM $MgCl_2$ and 1 mM EDTA for A_3), pH 7.4 and 100 μl of membranes and at least 12–14 different concentrations of typical adenosine receptor agonists and antagonists. Non-specific binding was defined as the binding in the presence of 1 μM DPCPX, SCH 58261 and MRE 3008F20 for A_1, A_{2A} and A_3, respectively and, at the K_D value for each radioligand, was about 30% of total binding. Bound and free radioactivity were separated by filtering the assay mixture through Whatman GF/B glass-fiber filters using a Micro-Mate 196 cell harvester (Packard Instrument Company). The filter bound radioactivity was counted on a Top Count Microplate Scintillation Counter (efficiency 57%) with Micro-Scint 20.

Measurement of cyclic AMP levels

A375 cells (5×10^6 cells/assay) were suspended in 0.5 ml of incubation mixture (mM): NaCl 150, KCl 2.7, NaH_2PO_4 0.37, $MgSO_4$ 1, $CaCl_2$ 1, glucose 5, HEPES 1, $MgCl_2$ 10, pH 7.4 at 37°C, containing 0.5 mM 4-(3-butoxy-4-methoxybenzyl)-2-imidazolidinone (Ro 20-1724) as phosphodiesterase inhibitor, 2.0 IU ml^{-1} adenosine deaminase and preincubated for 10 min in a shaking bath at 37°C. Then typical adenosine agonists plus forskolin (10 μM for A_1–A_3, 1 μM for A_{2A}–A_{2B}) were added to the mixture and incubated for a further 5 min. The reaction was terminated by the addition of cold 6% trichloroacetic acid (TCA). The TCA suspension was centrifuged at $2000 \times g$ for 10 min at 4°C and the supernatant was extracted four times with water-saturated diethyl ether. The final aqueous solution was tested for cyclic AMP levels by a competition protein binding assay carried out essentially according to Varani *et al*. (2000b). Samples of cyclic AMP standards (0–10 pmol) were added to each test tube containing Trizma base 0.1 M; aminophylline 8.0 mM; 2 mercaptoethanol 6.0 mM; pH 7.4 and [^{3}H]-cyclic AMP in a total volume of 0.5 ml. The binding protein, previously prepared from bovine adrenal glands, was added to the samples previously incubated at 4°C for 150 min. After the addition of charcoal the samples were centrifuged at $2000 \times g$ for 10 min. The clear supernatant (0.2 ml) was mixed with 4 ml of Atomlight and counted in a LS-1800 Beckman scintillation counter.

Calcium mobilization assays

Changes in [Ca^{2+}] were measured with the fluorescent indicator fura 2-AM, according to Varani *et al*., 2000b. Briefly, cells were loaded for 15 min with 4 μM fura 2-AM in HBS (mM): HEPES pH 7.4 20, NaCl 140, KCl 4, K_2HPO_4 1, $MgCl_2$ 1, $CaCl_2$ 1, D-glucose 10 and 0.1% BSA, buffer at 37°C. The cells were centrifuged at $1000 \times g$ for 10 min to remove extracellular dye and were resuspended in HBS buffer at 2×10^6 cells ml^{-1}. Fluorescence was monitored with a LS50, Perkin-Elmer, Norwalk, CT spectrofluorimeter in cuvettes thermostatically controlled at 37°C and continuously stirred.

Thermodynamic analysis

For a generic binding equilibrium L + R = LR (L = ligand, R = receptor), the affinity constant K_A is directly related to the standard free energy ΔG° ($\Delta G^\circ = -RT\ln K_A$) which can be separated in its enthalpic and entropic contributions according to the Gibbs equation: $\Delta G^\circ = \Delta H^\circ - T\Delta S^\circ$. ΔG° is calculated as $-RT\ln K_A$ at 25°C, while the determination of the other thermodynamic parameters (ΔH° and ΔS°) is performed by K_A measurements at different temperatures

($K_A = 1\ K_D^{-1}$ where K_D is the dissociation constant at equilibrium). Two general cases can be distinguished: (1) ΔCp° (the difference in standard specific heats at constant pressure of the equilibrium) is nearly zero. In this case, the equation $(\delta \ln K_a)/\delta\ (1\ T^{-1}) = -\Delta H^\circ\ R^{-1}$ gives a linear van't Hoff plot ln K_A versus (1/T) and standard enthalpy can be calculated from its slope, $-\Delta H^\circ\ R^{-1}$, while standard entropy is calculated as $\Delta S^\circ = (\Delta H^\circ - \Delta G^\circ)T^{-1}$ with T = 298.15 K and R = 8.314 J mol^{-1} K^{-1}; (2) ΔCp° is different from zero. The plot ΔG° versus T is often parabolic and other mathematical methods (Gilli *et al*., 1994) for calculating the thermodynamic parameters of the equilibrium are available. Saturation experiments of [^{3}H]-DPCPX, [^{3}H]-SCH 58261 and [^{3}H]-MRE 3008F20 binding to the human A_1, A_{2A} and A_3, respectively, were carried out at 4, 10, 20 and 25°C, in a thermostatic bath assuring a temperature of ± 0.1°C, using concentrations ranging from 0.5–30 nM. In the present case, the van't Hoff plot can be considered as being essentially linear and the first method was applied.

Data analysis and statistics

For saturation binding experiments, determination of receptor affinity (K_D) and receptor density (B_{MAX}) was performed using the non linear least-squares curve fitting program LIGAND (Munson & Rodbard, 1980). LIGAND was also used to determine inhibitory binding constant (K_I) values from the competition binding experiments. EC_{50} and K_I values were expressed as geometric means with 95% confidence intervals (CI). All other data are expressed as arithmetic mean ± s.e.mean. Unless otherwise stated, data are represented by three separate experiments, done in triplicate.

Results

RT–PCR

Total cDNA obtained from the human malignant melanoma A375 cell line was amplified with specific primers for β-actin and the obtained 654 bp product was run in agarose gel and is shown in Figure 1, lane 6. To exclude the presence of residual DNA contamination, RNA was directly amplified with β-actin primers and, as reported in lane 7, we did not find the amplified product confirming the absence of DNA contamination. So we amplified reverse-transcribed RNAs of A_1 (lane 2), A_{2A} (lane 3), A_{2B} (lane 4) and A_3 (lane 5) adenosine receptors. Detectable amounts of message for all four adenosine receptor subtypes were found.

Kinetic studies

Association studies indicated that equilibrium was reached after approximately 120, 90 and 150 min for [^{3}H]-DPCPX, [^{3}H]-SCH 58261 and [^{3}H]-MRE 3008F20, respectively, and was stable for at least 5 h (Figure 2A–C). [^{3}H]-DPCPX, [^{3}H]-SCH 58261 and [^{3}H]-MRE 3008F20 binding was rapidly reversed by the addition of 1 μM DPCPX, SCH 58261 and MRE 3008F20, respectively, as shown in Figure 2D–F. A two-site fit of association and dissociation curves was not significantly better than a one-site fit ($P < 0.05$). The rate constants were $k_{obs} = 0.0193 \pm 0.0005$, 0.0253 ± 0.0008, 0.0220 ± 0.0004 min^{-1} and $k_{-1} = 0.0136 \pm 0.0007$, 0.0161 ± 0.0004, 0.0145 ± 0.0005 min^{-1} from a $t_{1/2} = 36$, 31 and 49 min, for A_1, A_{2A} and A_3, respectively. With these values, kinetic dissociation constants (K_D) of 4.8, 7.0 and 7.7 nM, for A_1, A_{2A} and A_3, respectively, were calculated.

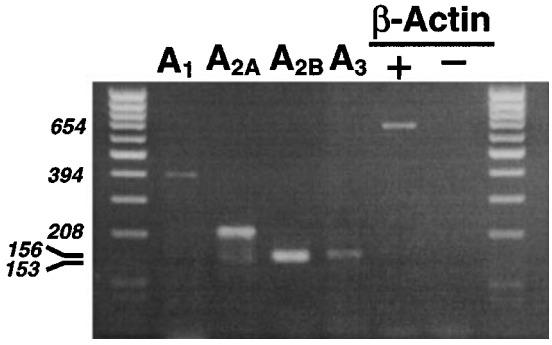

Figure 1 Expression of the adenosine receptors and β-actin transcripts in A375 cells. The PCR product in lane 2 is 394 bp long according to the human A_1 receptor sequence, that in lane 3 is 208 bp long according to the human A_{2A} receptor sequence, that in lane 4 is 153 bp long according to the human A_{2B} receptor sequence and that in lane 5 is 156 bp long according to the human A_3 receptor sequence. Lane 6 is 654 bp long according to the human β-actin sequence. Lanes 1 and 8 are molecular weight markers. Total RNA was extracted as described in Methods and used for RT–PCR (lanes 2–6) or directly used for PCR to detect β-actin DNA contaminant sequences (lane 7). Ten μl of PCR product were loaded in each lane. RT–PCR products obtained from A375 cells and separated on a 2% agarose gel.

Saturation studies

The expression of adenosine receptors in A375 cells was determined performing saturation binding experiments with [^{3}H]-DPCPX, [^{3}H]-SCH 58261 and [^{3}H]-MRE 3008F20 to label A_1, A_{2A} and A_3 receptors, respectively. A single saturable binding site was detected for all adenosine receptors. Saturation of [^{3}H]-DPCPX shows a K_D value of 1.9 ± 0.2 nM and B_{max} of 23 ± 7 fmol mg^{-1} of protein (Figure 3A). [^{3}H]-SCH 58261 exhibits high affinity for A_{2A} receptors with a K_D value of 5.1 ± 0.2 nM and B_{max} of 220 ± 7 fmol mg^{-1} of protein (Figure 3B). Figure 3C reports a saturation curve of [^{3}H]-MRE 3008F20 to the adenosine A_3 receptor with a K_D value of 3.3 ± 0.7 nM and B_{max} value of 291 ± 50 fmol mg^{-1} protein.

Competition studies

Competition curves for [^{3}H]-DPCPX binding of various agonists of adenosine receptors were best fitted assuming a two-state model corresponding to a high and low affinity state of the A_1 adenosine receptor (Figure 4A), a phenomenon expected for a G-protein-coupled receptor. Affinities are reported in Table 1 as K_I, K_H and K_L values, and the percentage of receptors in the high affinity state (R_H) is also shown. To test whether the high affinity state of the A_1 receptor was linked to a guanine nucleotide regulatory protein, the effect of GTP on the affinity states was examined. The presence of 100 μM GTP shifted the competition curves with agonists from a biphasic to a monophasic shape (LIGAND, $P < 0.01$), with a K_I close to the low affinity

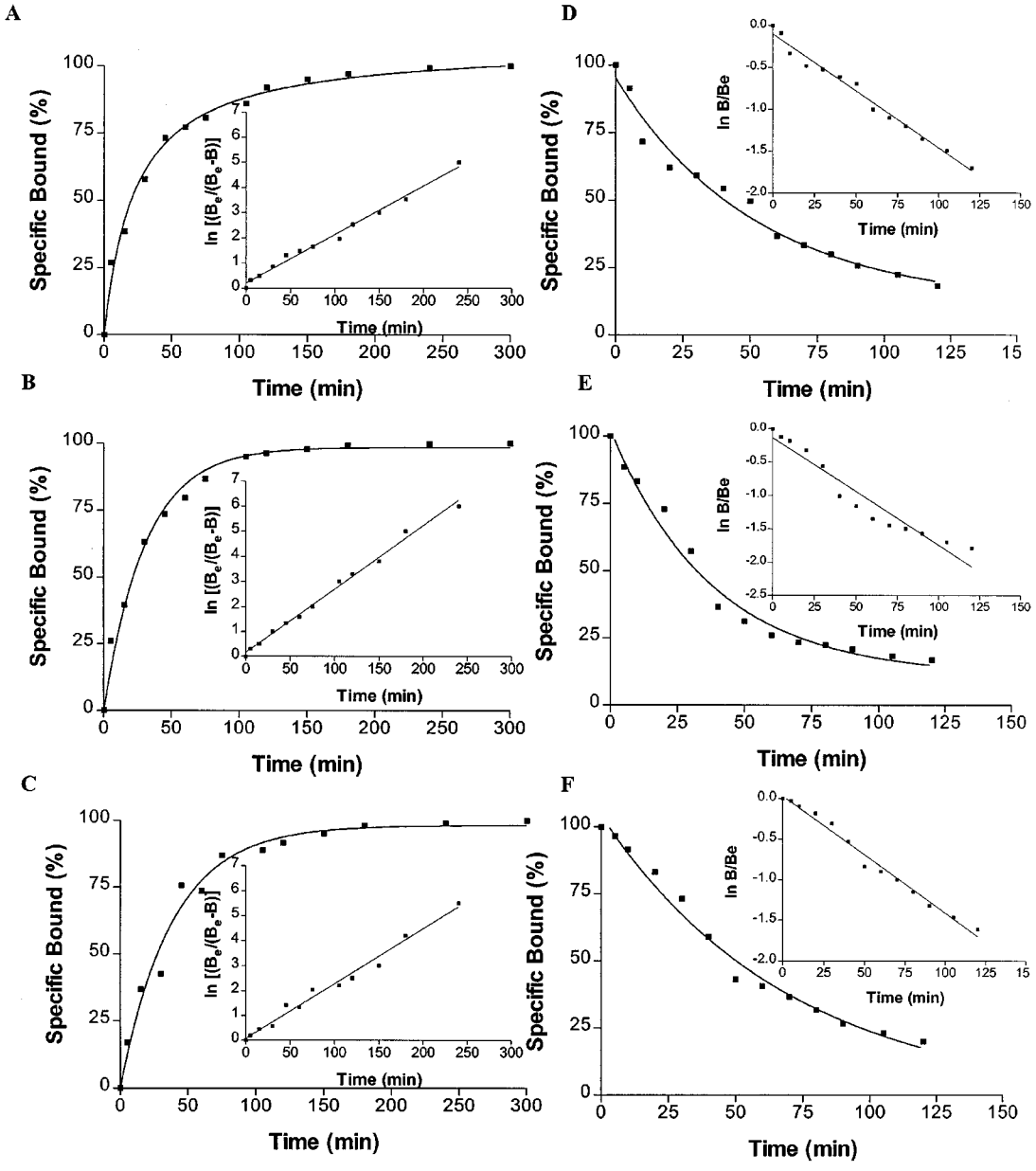

Figure 2 (A–C) Kinetics of [^{3}H]-DPCPX, [^{3}H]-SCH 58261 and [^{3}H]-MRE 3008F20 binding to human A_1, A_{2A} and A_3 adenosine receptors in A375 cells with association curves representative of a single experiment, which was replicated three times with similar results. The inset shows the data transformed as a semi-log plot, where B_e is the specific binding measured at equilibrium and B is the specific binding at time *t*. (D–F) Kinetics of [^{3}H]-DPCPX, [^{3}H]-SCH 58261 and [^{3}H]-MRE 3008F20 binding to human A_1, A_{2A} and A_3 adenosine receptors in A375 cells with dissociation curves representative of a single experiment, which was replicated three times with similar results. The inset shows the data transformed as a semi-log plot, where B is the specific binding at time t and B_e is the specific binding measured at equilibrium.

sites, as shown in Table 1. In contrast the above treatment did not change the shape of the competition curves with antagonists. The rank order of potency of adenosine agonists to compete with [^{3}H]-DPCPX binding to A375 membranes was: CPA > CHA > MECA > R-PIA > S-PIA. Competition of [^{3}H]-DPCPX was stereoselective, with R-PIA being approximately 73 times more active than its stereoisomer, S-PIA. The order of potency of the receptor antagonists to compete with [^{3}H]-DPCPX was: DPCPX > CPT > 8PT > SCH 58261 > MRE 3008F20. The selective A_1 receptor antagonist DPCPX displayed high affinity value, being the most potent antagonist compound.

K_I values for a series of adenosine receptor agonists and antagonists obtained in the competition of [^{3}H]-SCH 58261 binding are summarized in Table 2. Figure 4C,D shows the competition curves of adenosine agonists and antagonists in human malignant melanoma A375 membranes, respectively. The rank order of potency of adenosine agonists to compete with [^{3}H]-SCH 58261 binding to A375 membranes was: HE-NECA > NECA > CGS 21680 > R-PIA > CHA > S-PIA. The order of potency of the receptor antagonists to compete with [^{3}H]-SCH 58261 was: CGS 15943 > SCH 58261 > MRE 3008F20 > DPCPX. HE-NECA and NECA were the most potent agonists, their affinity being in the low nanomolar

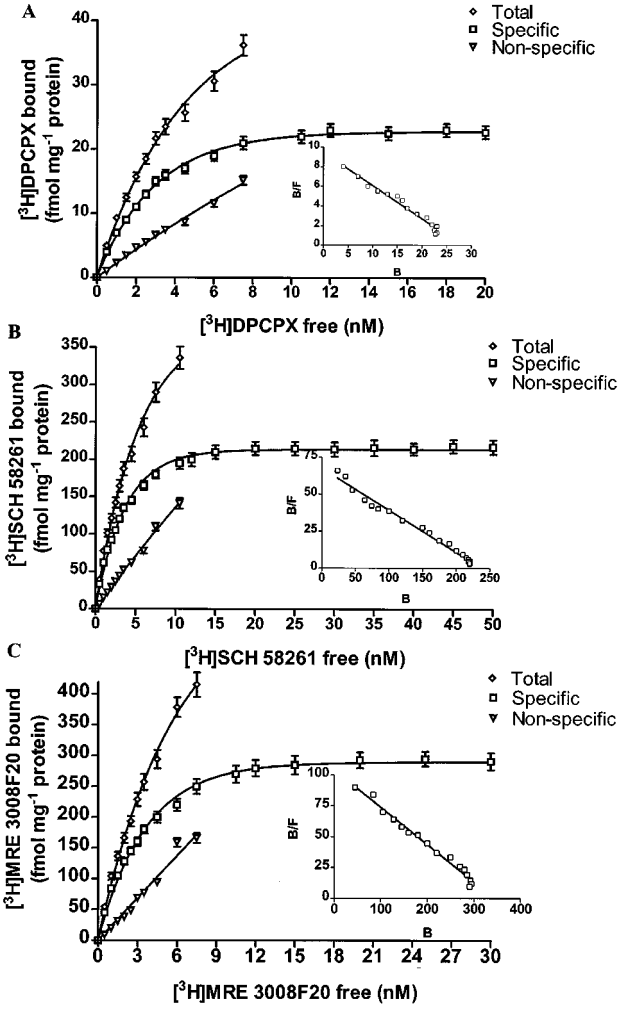

Figure 3 Saturation of [^{3}H]-DPCPX, [^{3}H]-SCH 58261 and [^{3}H]-MRE 3008F20 binding to A_1, A_{2A} and A_3 adenosine receptors in A375 cells. Experiments were performed as described in Methods. Values are the means and vertical lines s.e. of the mean of four separate experiments performed in triplicate. In the inset the Scatchard plot of the same data is shown.

range, while the selective A_1 receptor antagonist DPCPX displayed the worst affinity value. CGS 15943 and SCH 58261 were the most potent antagonist compounds. Competition of [^{3}H]-SCH 58261 was stereoselective, with R-PIA being approximately 14 times more active than its stereoisomer, S-PIA. Hill coefficients of all compounds were not significantly different from unity (data not shown).

Table 3 shows the comparison of affinities, expressed as K_I, K_H and K_L values, of selected adenosine receptor agonists and antagonists to human A_3 receptor expressed in A375 cells using [^{3}H]-MRE 3008F20, and the percentage of receptors in the high affinity state (R_H) is also shown. Only one affinity state could be detected with a slope factor near unity in the presence of GTP. The order of potency in [^{3}H]-MRE 3008F20 inhibition assays for adenosine receptor agonists resulted to be: Cl-IB-MECA > IB-MECA > HE-NECA > NECA > R-PIA > S-PIA. R-PIA was approximately six times more active (K_H = 40 nM; K_L = 2400 nM) than its stereoisomer, S-PIA (K_H = 240 nM; K_L = 23000 nM) showing the stereoselectivity of PIA binding. Antagonist competition curves for [^{3}H]-MRE 3008F20 binding gave the following rank order of potency: MRE 3055F20 > MRE 3062F20 > MRE 3048F20 > MRE 3046F20 > MRE 3008F20 > CGS 15943 > DPCPX each of which exhibited Hill slopes near to unity, either in the absence or in the presence of GTP (Figure 4F, Table 3). SCH 58261 showed a K_1 value > 10 μM.

Assay of cyclic AMP levels

Functional coupling of the A_{2A} adenosine receptors in A375 cells to adenylyl cyclase was investigated by measuring cyclic AMP production in response to HE-NECA, NECA and CGS 21680 as A_{2A} receptor agonists. All these agonists were able to increase cyclic AMP levels displaying an order of potency similar to that observed in binding affinities for the adenosine A_{2A} receptor. HE-NECA appeared to be the most potent compound (EC_{50} = 28 nM (95% CI: 23–34; n = 4) followed by NECA and CGS 21680 (EC_{50} = 131 nM (95% CI: 90–190, n = 4) and 246 nM (95% CI:190–320; n = 4), respectively) (Figure 5). The selective A_{2A} antagonist SCH 58261 (100 nM) totally inhibited the rise in cyclic AMP levels induced by HE-NECA and NECA (100 nM).

Functional coupling of the A_{2B} adenosine receptors in A375 cells to adenylyl cyclase was also investigated. We repeated the concentration-response curve of NECA-induced cyclic AMP accumulation in the presence of SCH 58261 100 nM, a concentration that produced maximal blockade of A_{2A} receptors while leaving A_{2B} receptors intact. The concentration-response curve of NECA + SCH 58261 100 nM (Figure 5B) was a typical sigmoidal curve with EC_{50} = 1206 nM (95% CI: 879–1655, n = 4) consistent with the presence on surface membranes of functional A_{2B} receptors.

The A_1 receptor agonist, CHA, and Cl-IB-MECA and IB-MECA, potent and selective A_3 agonists, in the range 0.1–10.000 nM, failed to significantly decrease cyclic AMP levels following stimulation with 10 μM forskolin, in the absence and in the presence of SCH 58261 (100 nM).

Calcium mobilization assays

The A_3 receptor agonist, Cl-IB-MECA, was able to stimulate Ca^{2+} release in A375 cells (Figure 6A) producing a rapid rise followed by a sustained increase in $[Ca^{2+}]_i$. Chelation of extracellular Ca^{2+} with EGTA (500 μM) did not influence the initial rise in $[Ca^{2+}]_i$ but abolished a second phase of elevations in $[Ca^{2+}]_i$, suggesting that the first rapid increase was due to Ca^{2+} release from intracellular Ca^{2+} pools, while the second phase of elevation appeared to result from an influx of extracellular Ca^{2+}. A375 cells responded to Cl-IB-MECA in a concentration dependent way with a calculated EC_{50} of 24 μM (95% CI: 19–32; n = 4) (Figure 6B). IB-MECA and NECA were also able to produce increases in $[Ca^{2+}]_i$ levels but in a higher range of concentrations, according to their order of potency in binding experiments performed in A375 cells. To verify the adenosine receptor subtype mediating the Cl-IB-MECA-induced calcium response, the effect of pre-incubation for 10 min with different antagonists of A_1 (DPCPX), A_{2A} (SCH 58261), A_{2A}/A_{2B} (ZM 241385) or A_3 (MRE 3008F20) adenosine receptors on Cl-IB-MECA-(10 μM)-stimulated calcium influx was evaluated. DPCPX, SCH 58261 and ZM 241385 were used at

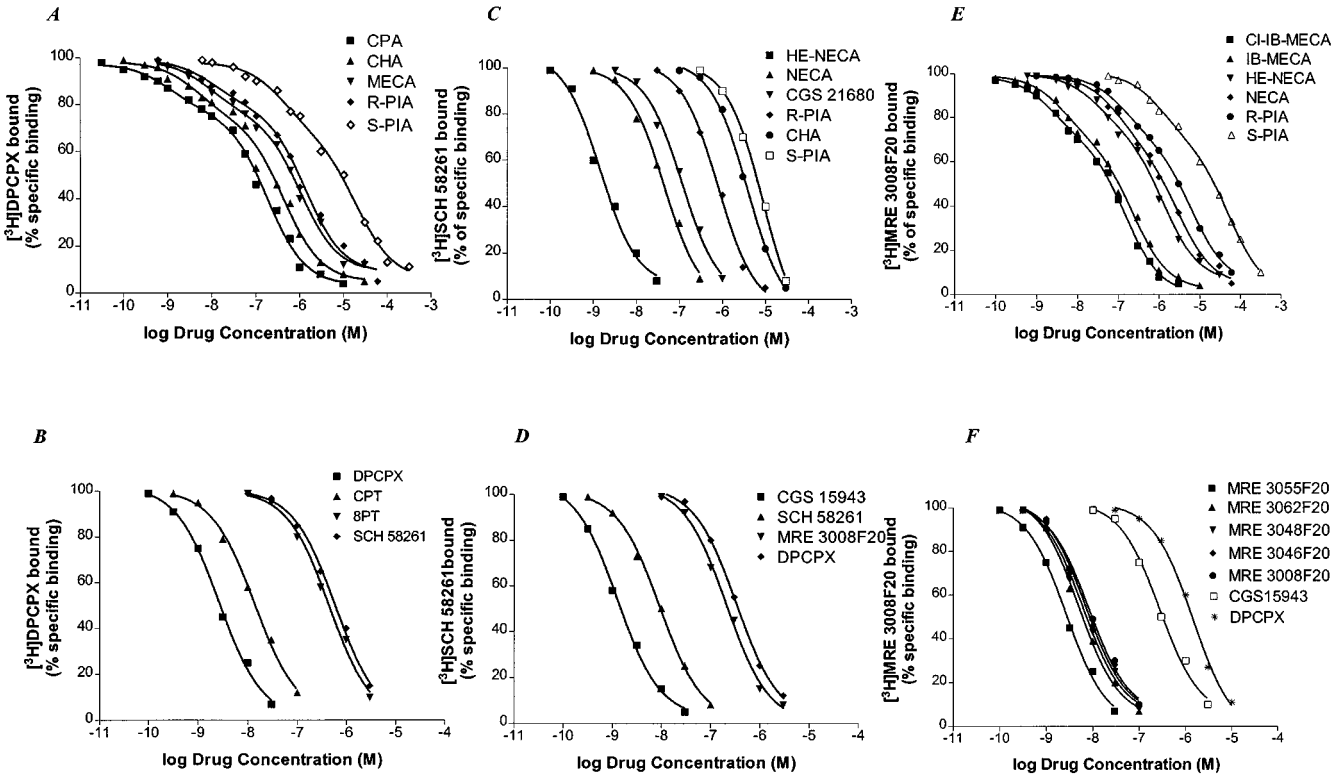

Figure 4 Competition curves of specific [^{3}H]-DPCPX, [^{3}H]-SCH 58261 and [^{3}H]-MRE 3008F20 binding to human A_1, A_{2A} and A_3 adenosine receptors in A375 cells by adenosine agonists (A,C,E) and antagonists (B,D,F). Curves are representative of a single experiment from a series of four independent experiments. Competition experiments were performed as described in Methods.

Table 1 Inhibition of [^{3}H]-DPCPX (K_H, K_L, K_I) binding by adenosine agonists and antagonists to human melanoma A375 membranes

Agonists	*[^{3}H]-DPCPX binding* (K_H, K_L)[a] *nM*	R_H (%)[b]	*[^{3}H]-DPCPX binding* (K_i) *nM + GTP*
CPA	0.050 (0.038–0.066)	22±3	
	90 (68–120)		87 (61–123)
CHA	0.20 (0.15–0.26)	26±2	
	129 (89–187)		125 (89–176)
MECA	1.6 (1.3–1.9)	25±5	
	847 (835–859)		853 (835–872)
R-PIA	2.1 (1.3–3.2)	22±3	
	942 (706–1258)		977 (599–1595)
S-PIA	154 (114–207)	33±4	
	7637 (5722–10194)		7709 (5080–11696)
Antagonists	*[^{3}H]DPCPX binding* (K_i) *nM*		*[^{3}H]DPCPX binding* (K_i) *nM + GTP*
DPCPX	1.9 (1.3–2.8)		1.8 (1.6–2.0)
CPT	7.0 (6.3–7.8)		6.3 (5.8–6.9)
8PT	133 (92–192)		126 (91–175)
SCH58261	198 (140–281)		204 (155–269)
MRE 3008F20	>1 μM		>1 μM

[a]K_H and K_L are the K_i values of the high and low affinity states for agonists, respectively. K_H and K_L values are expressed as geometric means with 95% confidence intervals and [b]R_H values (the percentage of A_1 receptors in the high affinity state) as mean±standard error of four separate experiments.

Table 2 Inhibition of [^{3}H]-SCH 58261 binding (K_I) by adenosine agonists and antagonists to human melanoma A375 membranes

	[^{3}H]-SCH 58261 binding K_i *(nM)*
Agonists	
HE-NECA	0.9 (0.7–1.2)
NECA	32 (24–42)
GCS 21680	63 (45–88)
R-PIA	436 (294–647)
CHA	2470 (1744–3498)
S-PIA	6233 (4478–8674)
Antagonists	
CGS 15943	0.11 (0.06–0.22)
SCH 58261	5.1 (4.4–5.9)
MRE 3008F20	126 (91–174)
DPCPX	188 (133–265)

K_i values are expressed as geometric means with 95% confidence intervals of four separate experiments.

0.1 μM because at this concentration they selectively block A_1, A_{2A} and A_{2A}/A_{2B} receptors, respectively. These antagonists did not prevent Cl-IB-MECA mediated calcium influx, whereas the A_3 antagonist MRE 3008F20 at the same concentration (0.1 μM) reduced calcium levels by 30±3%. Furthermore, 1 μM MRE 3008F20 completely abolished Cl-IB-MECA induced calcium influx (data not shown).

Table 3 Inhibition of [^{3}H]-MRE 3008F20 (K_H, K_L, K_i) binding by adenosine agonists and antagonists to human melanoma A375 membranes

Agonists	*[^{3}H]-MRE 3008F20 binding* (K_H, K_L)[a] *nM*	R_H (%)[b]	*[^{3}H]-MRE 3008F20 binding* (K_i) *nM* + *GTP*
C1-IB-MECA	0.5 (0.3–0.7)	29±4	
	81 (59–110)		89 (65–121)
IB-MECA	1.3 (1.1–1.5)	31±5	
	148 (105–210)		133 (93–189)
HE-NECA	10 (8–12)	26±5	
	723 (531–985)		593 (419–839)
NECA	22 (14–33)	33±4	
	1656 (984–2787)		1983 (1486–2647)
R-PIA	39 (24–63)	30±5	
	2380 (1774–3193)		2074 (1446–2974)
S-PIA	237 (170–331)	31±6	
	22602 (14807–34500)		25695 (18160–36355)
Antagonists	*[^{3}H]-MRE 3008F20 binding* (K_i) *nM*		*[^{3}H]-MRE 3008F20 binding* (K_i) *nM* + *GTP*
MRE 3055F20	1.4 (1.2–1.6)		1.7 (1.5–1.9)
MRE 3062F20	2.3 (1.6–3.1)		2.1 (1.6–2.7)
MRE 3048F20	2.6 (1.8–3.9)		2.5 (1.7–3.6)
MRE 3046F20	3.0 (2.5–3.6)		3.1 (2.1–4.4)
MRE 3008F20	3.1 (2.1–4.4)		3.4 (2.6–4.4)
CGS 15943	118 (79–177)		99 (68–143)
DPCPX	1181 (788–1771)		1073 (647–1780)
SCH 58261	>10000		>10000

[a]K_H and K_L are the K_i values of the high and low affinity states for agonists, respectively. K_H and K_L values are expressed as geometric means with 95% confidence intervals and [b]R_H values (the percentage of A_3 receptors in the high affinity state) as mean±standard error of four separate experiments.

Thermodynamic analysis

K_D and B_{max} derived from the saturation experiments of [^{3}H]-DPCPX, [^{3}H]-SCH 58261 and [^{3}H]-MRE 3008F20 binding to A_1, A_{2A} and A_3 adenosine receptors performed at the four temperatures selected were found within the following range: K_D=1.3–1.9, 5.1–5.9 and 3.3–4.3 nM and B_{max}=23–25, 220–240 and 291–310 fmol mg^{-1} protein, for A_1, A_{2A} and A_3 receptors, respectively. While the dissociation constant (K_D) changed with temperature, B_{max} values obtained from [^{3}H]-DPCPX, [^{3}H]-SCH 58261 and [^{3}H]-MRE 3008F20 saturation experiments appeared to be independent of it. Figure 7A–C shows the van't Hoff plot lnK_A versus 1/T of the [^{3}H]-DPCPX, [^{3}H]-SCH 58261 and [^{3}H]-MRE 3008F20 binding to the A_1, A_{2A} and A_3 adenosine receptors, respectively, and the final equilibrium thermodynamic parameters (expressed as mean values±standard error of three independent determinations) are expressed in Table 4. The linearity of the plot was statistically significant (ΔCp°, equilibrium heat capacity change, ≈ 0) and its slope ($-\Delta H^\circ\ R^{-1}$) was positive for all receptors, a property which has been found to be typical for antagonist binding to adenosine receptors (Borea *et al*., 1996).

Discussion

The goal of the present study was the pharmacological and biochemical characterization of adenosine receptors in the human malignant melanoma A375 cell line.

We have firstly analysed the expression of the human adenosine receptors by checking the production of the RNA of all the adenosine receptors known. By RT–PCR we have detected the expression of the transcript of A_1, A_{2A}, A_{2B} and A_3 receptors. Furthermore, we have found strong differences on RNA expression being A_1 and A_3 mRNAs less expressed than A_{2A} and A_{2B} mRNAs. It should be noted that this result is not predictive of the presence of adenosine receptor in the membrane surface because posttranscriptional events can modulate the amount of protein. Thus, in the present study, we have characterized, for the first time, A_1, A_{2A} and A_3 adenosine receptors on A375 membranes by using the selective radioligands [^{3}H]-DPCPX, [^{3}H]-SCH 58261 and [^{3}H]-MRE 3008F20.

It is difficult to estimate the number of A_{2B} receptors expressed in A375 cells because selective ligands for ligand-binding studies are not available. Recently, the new xanthine derivative antagonist MRS 1754 was characterized as a selective antagonist tritiated radioligand for A_{2B} receptors (Ji *et al*., 2001). Unfortunately, this radioligand is not commercially available. In this light, a pharmacological characterization of this adenosine receptor subtype has not been performed.

To investigate the kinetic behaviour, the binding was carried out under pseudo-first order conditions. Analysis of association and dissociation kinetic parameters produced equilibrium constants for A_1, A_{2A} and A_3 which are in good agreement with those obtained from the equilibrium saturation binding assays.

In saturation experiments the antagonist [^{3}H]-DPCPX labelled a single saturable binding site with a good affinity but with a low receptor density (B_{max}=23±7 fmol mg^{-1} of protein) while the radiolabelled [^{3}H]-SCH 58261 identified a large number (B_{max}=220±7 fmol mg^{-1} of protein) of high-affinity binding sites in A375 membranes. At the same time,

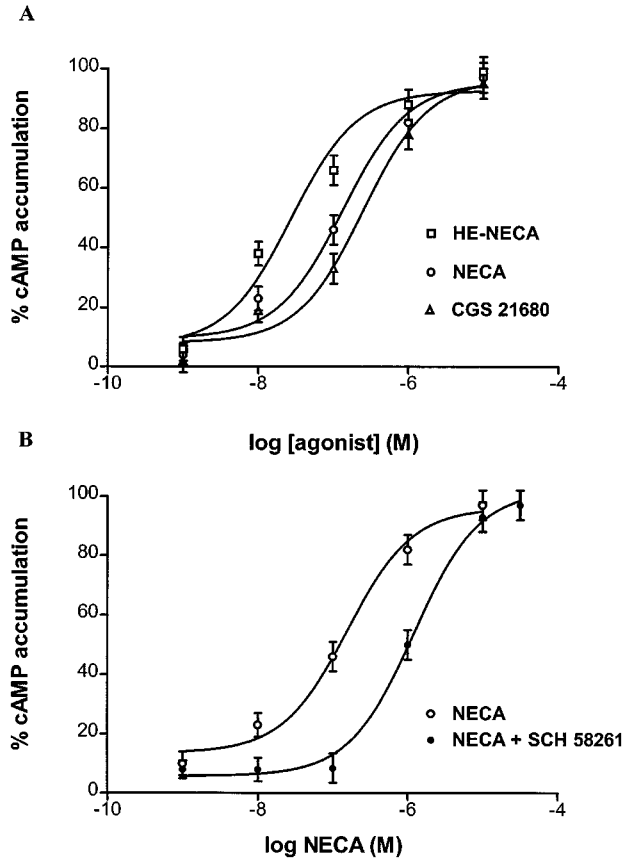

Figure 5 Stimulation curves of cyclic AMP levels by HE-NECA, NECA and CGS 21680 in A375 cells (A). Effect of increasing concentrations of NECA on cyclic AMP accumulation in A375 cells in the absence and in the presence of 100 nM A_{2A} selective antagonist SCH 58261 (B). Data (mean of three experiments ± s.e.mean) are given in percentages.

[^{3}H]-MRE 3008F20 labelled a single class of recognition sites with binding capacity (B_{max}) of 291 ± 50 fmol mg^{-1} protein. Interestingly, despite the ability to transcribe A_{2A} and A_3 adenosine receptor genes at different levels, A375 cells present on the membrane surface similar amounts of receptor protein. Thus, we have performed a more detailed pharmacological and biochemical characterization for A_1, A_{2A} and A_3 receptor subtypes with the aim of increasing the evidences in support of the conclusion that the [^{3}H]-DPCPX, [^{3}H]-SCH58261 and [^{3}H]-MRE 3008F20 binding sites in melanoma membranes are A_1, A_{2A} and A_3 receptors. This goal comes from the results of competition binding assays and functional studies. As illustrated in Figure 4 and summarized in Tables 1–3, the agonist and antagonist affinities for [^{3}H]-DPCPX, [^{3}H]-SCH58261 and [^{3}H]-MRE 3008F20 binding sites are consistent with the identification of these sites as A_1, A_{2A} and A_3 (Gessi *et al*., 2000; Varani *et al*., 2000a).

Competition of [^{3}H]-DPCPX by increasing concentrations of CPA, CHA, MECA, R-PIA and S-PIA (Table 1 and Figure 4A) revealed two binding sites for these agonists. The addition of GTP (100 μM) and subsequent uncoupling of receptors from G-proteins converted the curves of agonists from biphasic to monophasic. The similarity between K_i values determined in the presence of GTP and K_L values obtained in the absence of GTP indicated a guanine nucleotide-mediated shift of the high affinity binding sites to a low affinity form, a finding in agreement with that reported for human A_3 receptors transfected in CHO cells (Varani *et al*., 2000a). On the contrary, competition binding curves with antagonists were monophasic and did not change by the addition of GTP, indicating that antagonists bind equally well to both receptor states, whereas agonists discriminate between them.

HE-NECA, NECA and CGS 21680, A_{2A} agonists, were significantly more potent than the A_1 agonists R-PIA and CHA to compete with [^{3}H]-SCH 58261 for binding sites. Also, unlabelled SCH 58261 was significantly more potent than the A_1 antagonist DPCPX. Coupling of the A_{2A} receptor to its G protein is tight (Palmer & Stiles, 1995; Varani *et al*., 1997). Hence, we did not perform competition experiments of agonists with [^{3}H]-SCH 58261 binding in the presence of GTP because there is only slow dissociation of agonists from the receptor. The results of radioligand binding studies were consistent with the results of functional assays. We evaluated EC_{50} values obtained for the stimulation by HE-NECA, NECA and CGS 21680 of cyclic AMP levels. Interestingly, in the adenylyl cyclase assay, the compounds examined exhibited a rank order of potency very close to that observed in binding experiments. The block obtained in the presence of the selective A_{2A} antagonist SCH 58261 in the increase of cyclic AMP levels induced by HE-NECA and NECA (100 nM) suggested that the stimulatory effect was essentially A_{2A}-mediated.

To verify the expression of functional A_{2B} receptors, we used the approach previously described by Feoktistov & Biaggioni, 1998. The non-selective agonist NECA can be used in conjunction with highly selective antagonists of other adenosine receptor subtype to selectively stimulate A_{2B} receptors in cell systems where different adenosine receptors are coexpressed. Thus, the selective A_{2A}-antagonist SCH 58261 can be useful in the discrimination of A_{2B} function in A375 cells also coexpressing A_{2A} receptors. Figure 5B shows an unequivocally A_{2B}-mediated cyclic AMP response. These data indicate that the human melanoma A375 cells express an A_{2B}-adenosine receptor coupled positively to adenylyl cyclase.

Agonists competition of [^{3}H]-MRE 3008F20 yielded both a high and low-affinity state of the A_3 receptor (Figure 5A). After uncoupling the A_3 adenosine receptor from G proteins by GTP 100 μM treatment, binding of A_3 agonists was to a single low-affinity state, identical to the binding of antagonists (Table 3), including a series of new substituted pyrazolo triazolo pyrimidines (Baraldi *et al*., 1999; Baraldi & Borea, 2000).

We found a lack of effectiveness of CHA, A_1 agonist, and Cl-IB-MECA and IB-MECA, A_3 agonists, to significantly decrease cyclic AMP levels following stimulation with forskolin. It may be suggested that the effect on the stimulation of cyclic AMP levels by A_{2A} receptors prevailed over the A_1- and A_3-mediated inhibitory actions, suggesting a stronger potency of A_{2A} receptors in signal transduction over the A_1 and A_3 receptors. Furthermore, in our experience, we have observed that the co-expression of receptors coupled with Gs proteins and receptors coupled with Gi proteins can mask adenylyl cyclase inhibitor activity of Gi coupled receptors. Our observations agree according to the signalling consequences obtained in doubly Gs/Gi-coupled chimaeric

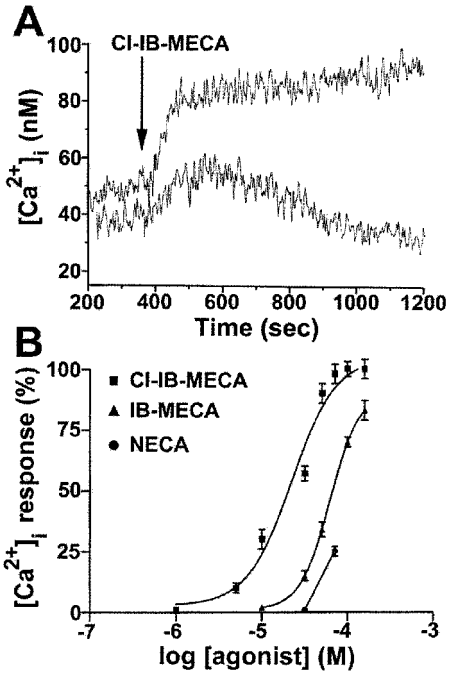

Figure 6 Effect of Cl-IB-MECA (30 μM) on intracellular calcium mobilization. Lower trace was obtained in calcium free medium and in the presence of 0.5 mM EGTA (A). Concentration dependent stimulation of Ca^{2+} mobilization by Cl-IB-MECA, IB-MECA and NECA in A375 cells (B). Data (mean of three experiments ± s.e.mean) are given in percentages.

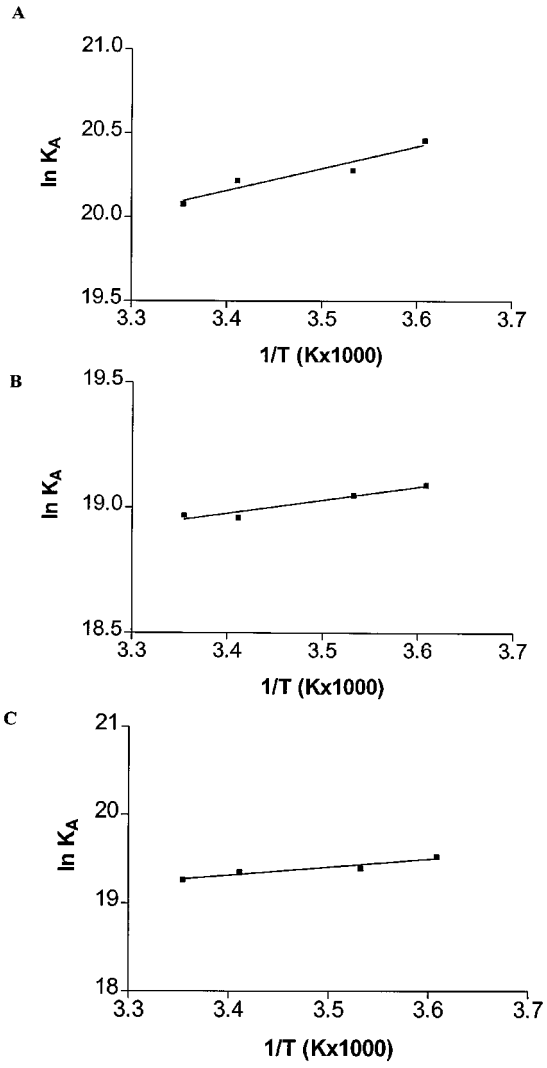

Figure 7 Van't Hoff plot showing the effect of temperature on the equilibrium binding association constant, $K_A = 1/K_D$ of [^{3}H]-DPCPX, [^{3}H]-SCH 58261 and [^{3}H]-MRE 3008F20. The plot is essentially linear in the temperature range investigated 4–25°C.

A_1/A_{2A} adenosine receptors in HEK-293 cells (Tucker *et al.*, 2000). Furthermore, it is note worthy that it could well be that an adenylyl cyclase inhibition could not be detected because the selectivity that is found in binding is often not found in functional assays and, thus, stimulation and inhibition of the cyclase may occur at very similar concentrations. Thus, in order to exclude the A_{2A} interference on A_1-A_3 signalling, we tested A_1 and A_3 agonists also in the presence of SCH 58261 aiming to block A_{2A} receptors, but we did not find any effect in adenylyl cyclase inhibition. This could be explained recognizing that the magnitude of the cyclic AMP response depends not only on the number of receptors but also on the amount of available G protein and the activity of the effector enzyme (Arslan *et al.*, 1999). In addition, it may be suggested that A_1 and A_3 receptors in A375 cells are not efficiently coupled to Gi proteins. In particular, A_1 undetectable effects on adenylyl cyclase activity may be the consequence of its low expression on cell surface.

In calcium mobilization studies, the A_3 agonist Cl-IB-MECA was able to increase $[Ca^{2+}]_i$ (Figure 6A). EC_{50} value for this agonist was largely different if compared with its affinity determined in binding studies, according to that obtained in other cell systems (Abbracchio *et al.*, 1995; Brambilla *et al.*, 2000; Jacobson., 1998, Kohno *et al.*, 1996a,b; Varani *et al.*, 2000a; Gessi *et al.*, 2001). This discrepancy, previously noted, seems to be a common characteristic of the A_3 adenosine receptor but the reasons are not clearly known. We hypothesize that in a dynamic and complex cell system, A_3 receptor may interact, after agonist binding, with different types of G proteins that differ in their ability to couple to different regulatory signalling systems, as reported for A_{2A} receptors (Fredholm *et al.*, 2000). Pre-treatment of A375 cells with the A_3 antagonist MRE 3008F20 potently reduced the rise in intracellular calcium induced by a submaximal dose of Cl-IB-MECA. This block, not obtained with A_1-A_{2A}-A_{2B} receptor antagonists pre-treatment, suggested that the adenosine receptor subtype involved in the calcium response could be the A_3.

Finally, thermodynamic studies were performed and the enthalpic (ΔH°) and entropic (ΔS°) contributions to the standard free energy (ΔG°) of the binding equilibrium were determined. The linearity of the van't Hoff plot (Figure 7) indicates that ΔCp° values for the drug interaction are nearly zero, which means that ΔH° and ΔS° values are not significantly affected by temperature variations at least over the temperature range investigated (Borea *et al.*, 1996). It is notable that the linearity of van't Hoff plots in a limited range of temperatures (4–25°C) appears to be a common feature of practically all membrane receptor ligands so far studied from a thermodynamic point of view (Gilli *et al.*, 1994). Thermodynamic data obtained from the van't Hoff

Table 4 Thermodynamic parameters observed for the binding of [^{3}H]-DPCPX, [^{3}H]-SCH 58261 and [^{3}H]-MRE 3008F20 to A_1, A_{2A} and A_3 receptors in A375 membranes, respectively

Receptor	ΔG° (kJ mol^{-1})	ΔH° (kJ mol^{-1})	ΔS° (J mol^{-1} K^{-1})
A_1	-49.6 ± 2.4	-10.9 ± 1.3	130.0 ± 11.1
A_{2A}	-46.8 ± 3.2	-4.4 ± 0.8	142.2 ± 14.0
A_3	-47.6 ± 4.5	-7.6 ± 1.1	134.2 ± 10.6

All values are the mean $\pm$ standard error of four experiments.

plot indicate that [^{3}H]-DPCPX, [^{3}H]-SCH 58261 and [^{3}H]-MRE 3008F20 binding to human A_1, A_{2A} and A_3 receptors is enthalpy- and entropy-driven (Table 4). This binding behaviour has previously been found to be typical of adenosine A_1, A_{2A} and A_3 antagonists (Borea *et al*., 1996; Varani *et al*., 2000a). This is remarkable since the similarity in thermodynamic parameters may be the key for understanding the difficulty of obtaining selective adenosine receptor ligands. Although much progress has been made in recent years to synthesize potent and selective adenosine receptor ligands, today the result is that compounds exhibiting high affinity to only one subtype are an exception (Klotz, 2000).

In conclusion all these data indicate, for the first time, that adenosine receptors present on A375 melanoma cell line have a pharmacological and biochemical profile typical of the A_1, A_{2A}, A_{2B} and A_3 receptor subtype.

Recently, it has been reported that human tumoural Jurkat cell line expresses high level of A_3 receptors (Gessi *et al*., 2001) in agreement with our results in human melanoma cell line. Furthermore, it has been reported that A_3 adenosine receptors increase cell survival of rat leukaemia mast cells by triggering an antiapoptotic signalling (Gao *et al*., 2001). In our opinion, the presence of adenosine receptors in a malignant cell type, as melanoma, suggests a potential role for adenosine in modulating tumoural processes (Ohana *et al*., 2001). Given this, we propose the full characterization of adenosine receptors in tumour and normal tissue with the aim to elucidate if A_3 or a combination of different adenosine receptors could be associated to the development and promotion of malignant phenotype.

References

ABBRACCHIO, M.P., BRAMBILLA, R., CERUTI, S., KIM, H.O., VON LUBITZ, D.K.J.E., JACOBSON, K.A. & CATTABENI, F. (1995). G Protein-dependent activation of phospholipase C by adenosine A_3 receptors in rat brain. *Mol. Pharmacol.,* **48,** 1038 – 1045.

ARIZA, M.E., BROOME-POWELL, M., LAHTI, J.M., KIDD, V.J. & NELSON, M.A. (1999). Fas-induced apoptosis in human malignant melanoma cell lines is associated with the activation of the p34^{cdc2}-related PITSLRE protein kinases. *J. Biol. Chem.,* **274,** 28505 – 28513.

ARSLAN, G., KULL, B. & FREDHOLM, B.B. (1999). Signaling via A_{2A} adenosine receptor in four PC12 cell clones. *Naunyn Schmiedebergs Arch Pharmacol.,* **359,** 28 – 32.

BARALDI, P.G., CACCIARI, B., ROMAGNOLI, R., SPALLUTO, G., KLOTZ, K-N., LEUNG, E., VARANI, K., GESSI, S., MERIGHI, S. & BOREA, P.A. (1999). Pyrazolo[4,3-e]1,2,4-triazolo[1,5-c]-pyrimidine derivatives as highly potent and selective human A_3 adenosine receptor antagonists. A possible template for adenosine receptor subtypes? *J. Med. Chem.,* **42,** 4473 – 4478.

BARALDI, P.G., CACCIARI, B., ROMAGNOLI, R., VARANI, K., MERIGHI, S., GESSI, S., BOREA, P.A., LEUNG, E., HICKEY, S.L. & SPALLUTO, G. (2000). Synthesis and preliminary biological evaluation of [^{3}H]-MRE 3008-F20: the first high affinity radioligand antagonist for the human A_3 adenosine receptors. *Bioorg. Med. Chem. Lett.,* **10,** 209 – 211.

BARALDI, P.G. & BOREA, P.A. (2000). New potent and selective human adenosine A_3 receptor antagonists. *Trends Pharmacol. Sci.,* **21,** 456 – 459.

BLACKBURN, M.R., DATTA, S.K., WAKAMIYA, M., VARTABEDIAN, B.S. & KELLEMS, R.E. (1996). Metabolic and immunologic consequences of limited adenosine deaminase expression in mice. *J. Biol. Chem.*, **271,** 15203 – 15210.

BLAY, J., WHITE, T.D. & HOSKIN, D.W. (1997). The extracellular fluid of solid carcinomas contains immunosuppressive concentrations of adenosine. *Cancer Res.,* **57,** 2602 – 2605.

BOREA, P.A., DALPIAZ, A., VARANI, K., GESSI, S. & GILLI, G. (1996). Binding thermodynamics at A_1 and A_{2A} adenosine receptors. *Life Sci.,* **59,** 1373 – 1388.

BRADFORD, M.M. (1976). A rapid and sensitive method for the quantification of microgram quantities of protein utilizing the principle of protein dye-binding. *Anal. Biochem.,* **72,** 248 – 254.

BRAMBILLA, R., CATTABENI, F., CERUTI, S., BARBIERI, D., FRANCESCHI, C., KIM, Y.C., JACOBSON, K.A., KLOTZ, K.N., LOHSE, M.J. & ABBRACCHIO, M.P. (2000). Activation of the A_3 adenosine receptor affects cell cycle progression and cell growth. *Naunyn Schmiedebergs Arch Pharmacol.,* **361,** 225 – 234.

ELENKOV, I.J., CHROUSOS, G.P. & WILDER, R.L. (2000). Neuroendocrine regulation of IL-12 and TNF-alpha/IL-10 balance. Clinical implications. *Ann. N.Y. Acad. Sci.,* **917,** 94 – 105.

ETHIER, M.F., CHANDER, V. & DOBSON, J.G. (1993). Adenosine stimulates proliferation of human endothelial cells in culture. *Am. J. Physiol.,* **265,** H131 – H138.

ETHIER, M.F. & DOBSON, J.G. (1997). Adenosine stimulation of DNA synthesis in human endothelial cells. *Am. J. Physiol.,* **272,** H1470 – H1479.

FEOKTISTOV, I. & BIAGGIONI, I. (1998). Pharmacological characterization of adenosine A_{2B} receptors: studies in human mast cells co-expressing A_{2A} and A_{2B} adenosine receptor subtypes. *Biochem. Pharmacol.,* **55,** 627 – 633.

FOZARD, J.R., PFANNKUCHE, H.J. & SCHUURMAN, H.J. (1996). Mast cell degranulation following adenosine A_3 receptor activation in rats. *Eur. J. Pharmacol.,* **298,** 293 – 297.

FREDHOLM, B.B., ABBRACCHIO, M.P., BURNSTOCK, G., DALY, J.W., HARDEN, K., JACOBSON, K.A., LEFF, P. & WILLIAMS, M. (1994). VI: Nomenclature and classification of purinoceptors. *Physiol. Rev.,* **46,** 143 – 156.

FREDHOLM, B.B., ARSLAN, G., HALLDNER, L., KULL, B., SCHULTE, G. & WASSERMAN, W. (2000). Structure and function of adenosine receptors and their genes. *Naunyn Schmiedebergs Arch. Pharmacol.,* **362,** 364 – 374.

FREDHOLM, B.B., IRENIUS, E., KULL, B. & SCHULTE, G. (2001). Comparison of the potency of adenosine as an agonist at human adenosine receptors expressed in Chinese hamster ovary cells. *Biochem. Pharmacol.,* **61,** 443 – 448.

GAO, Z., LI, B.S., DAY, Y.J. & LINDEN, J. (2001). A_3 adenosine receptor activation triggers phosphorylation of protein kinase B and protects rat basophilic leukemia 2H3 mast cells from apoptosis. *Mol. Pharmacol.,* **59,** 76 – 82.

GESSI, S., VARANI, K., MERIGHI, S., ONGINI, E. & BOREA, P.A. (2000). A_{2A} adenosine receptors in human peripheral blood cells. *Br. J. Pharmacol.,* **129,** 2 – 11.

GESSI, S., VARANI, K., MERIGHI, S., MORELLI, A., FERRARI, D., LEUNG, E., BARALDI, P.A., SPALLUTO, G. & BOREA, P.A. (2001). Pharmacological and biochemical characterization of A_3 adenosine receptors in Jurkat T cells. *Br. J. Pharmacol.,* **134,** 116–126.

GILLI, P., FERRETTI, V., GILLI, G. & BOREA, P.A. (1994). Enthalpy-entropy compensation in drug-receptor binding. *J. Phys. Chem.,* **98,** 1515–1518.

GUIEU, R., BRUNET, P., SAMPOL, J., BECHIS, G., FENOUILLET, E., MEGE, J.L., CAPO, C., VITTE, J., IBRAHIM, Z., CARREGA, L., LERDA, D., ROCHAT, H., BERLAND, Y. & DUSSOL, B. (2001). Adenosine and hemodialysis in humans. *J. Investig. Med.,* **49,** 56–67.

JACOBSON, K.A., NIKODIJEVIC, O., SHI, D., GALLO-RODRIGUEZ, C., OLAH, M.E., STILES, G.L. & DALY, J.W. (1993). A role for central A_3 adenosine receptors. Mediation of behavioural depressant effects. *FEBS Lett.,* **336,** 57–60.

JACOBSON, K.A. (1998). Adenosine A_3 receptors: novel ligands and paradoxical effects. *Trends Pharmacol. Sci.,* **19,** 184–191.

JI, X., KIM, Y.C., AHERN, D.G., LINDEN, J. & JACOBSON, K.A. (2001). [^{3}H]MRS 1754, a selective antagonist radioligand for A_{2B} adenosine receptors. *Biochem. Pharmacol.,* **61,** 657–663.

KLOTZ, K.N. (2000). Adenosine receptors and their ligands. *Naunyn. Schmiedebergs. Arch. Pharmacol.,* **362,** 382–391.

KOHNO, Y., SEI, Y., KOSHIBA, M., KIM, H.O. & JACOBSON, K.A. (1996A). Induction of apoptosis in HL-60 human promyelocytic leukemia cells by adenosine A_3 receptor agonists. *Biochem. Biophys. Res. Commun.,* **219,** 904–910.

KOHNO, Y., JI, X., MAWHORTER, S.D., KOSHIBA, M. & JACOBSON, K.A. (1996B). Activation of A_3 adenosine receptors on human eosinophils elevates intracellular calcium. *Blood,* **88,** 3569–3574.

LIANG, B.T. & JACOBSON, K.A. (1998). A physiological role of the adenosine A_3 receptor: sustained cardioprotection. *Proc. Natl. Acad. Sci. U.S.A.,* **95,** 6995–6999.

MARSTON, H.M., FINLAYSON, K., MAEMOTO, T., OLVERMAN, H.J., AKAHANE, A., SHARKEY, J. & BUTCHER, S.P. (1998). Pharmacological characterization of a simple behavioral response mediated selectively by central adenosine A_1 receptors, using in vivo and in vitro techniques. *J. Pharmacol. Exp. Ther.,* **285,** 1023–1030.

MONTESINOS, M.C., GADANGI, P., LONGAKER, M., SUNG, J., LEVINE, J., NILSEN, D., REIBMAN, J., LI, M., JIANG, C.K., HIRSCHHORN, R., RECHT, P.A., OSTAD, E., LEVIN, R.I. & CRONSTEIN, B.N. (1997). Wound healing is accelerated by agonist of adenosine A_2 (Gαs–linked) receptors. *J.Exp.Med.,* **186,** 1615–1620.

MUNSON, P.J. & RODBARD, D. (1980). Ligand: a versatile computerized approach for the characterization of ligand binding systems. *Anal. Biochem.,* **107,** 220–239.

OHANA, G., BAR-YEHUDA, S., BARER, F. & FISHMAN, P. (2001). Differential effect of adenosine on tumor and normal cell growth: focus on the A_3 adenosine receptor. *J. Cell. Physiol.,* **186,** 19–23.

OLAH, M.E. & STILES, G.L. (1995). Adenosine receptor subtypes: characterization and therapeutic regulation. *Annu. Rev. Pharmacol. Toxicol.,* **35,** 581–606.

PALMER, T.M. & STILES, G.L. (1995). Adenosine receptors. *Neuropharmacology.,* **34,** 683–694.

RALEVIC, V. & BURNSTOCK, G. (1998). Receptors for purines and pyrimidines. *Pharmacol. Rev.,* **50,** 413–492.

SAFRAN, N., SHNEYVAYS, V., BALAS, N., JACOBSON, K.A., NAWRATH, H. & SHAINBERG, A. (2001). Cardioprotective effects of adenosine A_1 and A_3 receptor activation during hypoxia in isolated rat cardiac myocytes. *Mol. Cell. Biochem.,* **217,** 143–152.

SCHRIER, S.M., VAN TILBURG, E.W., VAN DER MEULEN, H., IJZERMAN, A.P., MULDER, G.J. & NAGELKERKE, J.F. (2001). Extracellular adenosine-induced apoptosis in mouse neuroblastoma cells: studies on involvement of adenosine receptors and adenosine uptake. *Biochem. Pharmacol.,* **61,** 417–425.

TUCKER, A.L., JIA, L.G., HOLETON, D., TAYLOR, A.J. & LINDEN, J. (2000). Dominance of Gs in doubly Gs/Gi-coupled chimaeric A_1/A_{2A} adenosine receptors in HEK-293 cells. *Biochem. J.,* **352,** 203–210.

VARANI, K., GESSI, S., DALPIAZ, A., ONGINI, E. & BOREA, P.A. (1997). Characterization of A_{2A} adenosine receptors in human lymphocyte membranes by [^{3}H]-SCH 58261 binding. *Br. J. Pharmacol.,* **122,** 386–392.

VARANI, K., MERIGHI, S., GESSI, S., KLOTZ, K.N., LEUNG, E., BARALDI, P.G., CACCIARI, B., ROMAGNOLI, R., SPALLUTO, G. & BOREA, P.A. (2000a). [^{3}H]MRE 3008F20: a novel antagonist radioligand for the pharmacological and biochemical characterization of human A_3 adenosine receptors. *Mol. Pharmacol.,* **57,** 968–975.

VARANI, K., PORTALUPPI, F., GESSI, S., MERIGHI, S., ONGINI, E., BELARDINELLI, L. & BOREA, P.A. (2000b). Dose and time effects of caffeine intake on human platelet adenosine A_{2A} receptors: functional and biochemical aspects. *Circulation,* **102,** 285–289.

WALKER, B.A., JACOBSON, M.A., KNIGHT, D.A., SALVATORE, C.A., WEIR, T., ZHOU, D. & BAI, T.R. (1997). Adenosine A_3 receptor expression and function in eosinophils. *Am. J. Resp. Cell. Mol. Biol.,* **16,** 531–537.

WALTHER, W., STEIN, U. & EDER, C. (1994). RNA analysis using miniprep RNA in reverse transcription PCR. *Biotechniques,* **17,** 674–675.

YAO, Y., SEI, Y., ABBRACCHIO, M.P., JIANG, J.L., KIM, Y.C. & JACOBSON, K. (1997). Adenosine A_3 receptor agonists protect HL60 and U-937 cells from apoptosis induced by A_3 antagonists. *Biochem. Biophys. Res. Comm.,* **232,** 317–322.

(Received June 26, 2001
Revised August 7, 2001
Accepted August 24, 2001)